MOLECULAR AND CELLULAR BIOLOGY, Mar. 2008, p. 1862–1872 Vol. 28, No. 5
0270-7306/08/$08.00+0 doi:10.1128/MCB.01589-07

Role of hPHF1 in H3K27 Methylation and Hox Gene Silencing▽

Ru Cao,[1,2] Hengbin Wang,[1,2]† Jin He,[1,2] Hediye Erdjument-Bromage,[3] Paul Tempst,[3] and Yi Zhang[1,2]*

Howard Hughes Medical Institute[1] and Department of Biochemistry and Biophysics, Lineberger Comprehensive Cancer Center,[2] University of North Carolina at Chapel Hill, Chapel Hill, North Carolina 27599-7295, and Molecular Biology Program, Memorial Sloan Kettering Cancer Center, 1275 York Avenue, New York, New York 10021[3]

Received 29 August 2007/Returned for modification 29 October 2007/Accepted 7 December 2007

Polycomb group (PcG) proteins are required for maintaining the silent state of the homeotic genes and other important developmental regulators. The silencing function of the PcG proteins has been linked to their intrinsic histone modifying enzymatic activities. The EED-EZH2 complex, containing the core subunits EZH2, EED, SUZ12, and RbAp48, functions as a histone H3K27-specific methyltransferase. Here we describe the identification and characterization of a related EED-EZH2 protein complex which is distinguished from the previous complex by the presence of another PcG protein, hPHF1. Consistent with the ability of hPHF1 to stimulate the enzymatic activity of the core EED-EZH2 complex in vitro, manipulation of mPcl1, the mouse counterpart of hPHF1, in NIH 3T3 cells and cells of the mouse male germ cell line GC1spg results in global alteration of H3K27me2 and H3K27me3 levels and Hox gene expression. Small interfering RNA-mediated knockdown of mPcl1 affects association of the Eed-Ezh2 complex with certain Hox genes, such as HoxA10, as well as Hox gene expression concomitant with an alteration on the H3K27me2 levels of the corresponding promoters. Therefore, our results reveal hPHF1 as a component of a novel EED-EZH2 complex and demonstrate its important role in H3K27 methylation and Hox gene silencing.

Polycomb group (PcG) and Trithorax group (TrxG) proteins are key components required for the maintenance of long-term repressive and active chromatin states, respectively (9). They have been shown to play an important role in the regulation of homeotic box (HOX) genes and other developmental and cell cycle regulatory genes. Biochemical and genetic studies have provided considerable evidence that PcG proteins function in multiprotein complexes. At least two PcG protein complexes with distinct biochemical properties have been characterized. The 2-MDa Polycomb repressive complex 1 (PRC1) is comprised of the core subunits Polycomb (PC), Polyhomeotic (PH), and the three ring domain-containing proteins RING1, RING2, and BMI-1, which possess H2A-K119 ubiquitin E3 ligase activity (29). The catalytic subunit has been mapped to RING2, while the presence of RING1 and BMI-1 can enhance the enzymatic activity (1, 2, 14). Components from the transcriptional machinery, including TBP (TATA-binding protein) and TATA box-binding protein-associated factors (TAFs), are also observed to associate with the PRC1 complex in *Drosophila melanogaster* (23), indicating that the interaction might provide a platform for PRC1 to function at promoters.

The EED-EZH2/PRC2 complex contains EZH2, SUZ12, EED, and RbAp48 and has been demonstrated to have intrinsic histone methyltransferase (HMTase) activity toward H3K27 (3, 6, 13, 18). Silencing of some Hox genes requires coordinated action of the two PcG complexes. The prerequisite of H3K27 methylation mediated by the PRC2 complex for the recruitment of the PRC1 complex, through the specific recognition of H3K27me3 by the chromo domain of the PC protein (8, 16), in some Hox genes provides evidence for the molecular basis of the coordinated action of these two PcG protein complexes (2). With regard to the PRC2 complex, the SET domain-containing protein EZH2 is the catalytic subunit responsible for H3K27 methylation. However, each of the other components of the complex is indispensable for the overall function of the complex. For example, SUZ12 is required for the minimum activity of the complex in vitro and genome-wide H3K27 di- and trimethylation in vivo (4, 22). In contrast, EED is required for all states of H3K27 methylation, including monomethylation (17). RbAp48, the mammalian homolog of Nurf55, has been reported to bind directly to helix 1 of histone H4, which is usually inaccessible within the nucleosome (27). In *Drosophila*, Nurf55 together with Su(z)12 is the minimal nucleosome-binding module of the Esc-E(z) complex to anchor the complex on the chromatin substrates (20). The four components have been demonstrated to be the functional core of the PRC2 complex.

In *Drosophila*, an association between E(z) and another PcG protein named Polycomblike (PCL) has been observed and PCL shares the same polytene staining pattern with E(z) (21, 26). Indeed, a 1-MDa Esc-E(z) complex containing PCL and the histone deacetylase RPD3 is present during early embryogenesis. The different composition of the Esc-E(z) complex may be involved in the silencing of different targets. PCL contains two plant homeodomain (PHD) domains, a motif present in many proteins involved in chromatin function, such as CHD3, Mi2, TRX, ASH1, and ASH2. It has recently been shown that PHD domains link histone methylation to active chromatin remodeling (24, 32). Multiple PCL homologs have been identified in mammals. For example, there are three

* Corresponding author. Mailing address: Department of Biochemistry and Biophysics, Lineberger Comprehensive Cancer Center, University of North Carolina at Chapel Hill, Chapel Hill, NC 27599-7295. Phone: (919) 843-8225. Fax: (919) 966-4330. E-mail: yi_zhang@med.unc.edu.

† Present address: Department of Biochemistry and Molecular Genetics, University of Alabama at Birmingham, Kaul Human Genetics Building, Room 402A, 720 South 20th St., Birmingham, AL 35394.

▽ Published ahead of print on 17 December 2007.

genes in the mouse genome that encode PCL homologs, namely mPcl1, mPcl2, and mPcl3.

Here we report the identification and functional characterization of a novel EED-EZH2 complex, which is distinguished from the previously characterized PRC2 complex by the presence of hPHF1, the closest human homolog of *Drosophila* PCL. By comparing the enzymatic activities of different EED-EZH2 complexes in the presence or absence of hPHF1, we show that hPHF1 positively regulates the H3K27 methyltransferase activity of the EED-EZH2 core complex in vitro. In addition, we demonstrate that the mouse homolog of hPHF1 is important for H3K27 methylation and Hox gene expression in vivo. Finally, chromatin immunoprecipitation (ChIP) assays demonstrate that mPcl1 directly contributes to HoxA10 silencing by facilitating the recruitment of the Eed-Ezh2 complex and subsequent H3K27 methylation at its promoter. Therefore, our study not only provides strong evidence that hPHF1 is an integral component of a novel EED-EZH2 complex, but also demonstrates its important function in H3K27 methylation and Hox gene silencing.

MATERIALS AND METHODS

Purification and identification of an hPHF1-containing EED-EZH2 complex. HeLa nuclear proteins were separated into nuclear extract and nuclear pellet fractions as previously described (28). After solubilization, proteins derived from nuclear pellets were resuspended in buffer D (50 mM Tris-HCl [pH 7.9], 0.1 mM EDTA, 2 mM dithiothreitol [DTT], 0.2 mM phenylmethylsulfonyl fluoride [PMSF], and 25% glycerol) containing 20 mM ammonium sulfate (BD20) and loaded onto a DEAE52 column equilibrated with BD20. Proteins bound to DEAE52 column were step eluted with BD350 and BD500. The BD350 fraction was dialyzed against buffer C (50 mM Tris-HCl [pH 7.9], 0.2 mM EDTA, 1 mM DTT, 0.2 mM PMSF, and 20% glycerol) containing 100 mM potassium chloride (BC100) and loaded onto a phosphocellulose P11 column. The column was step eluted with BC300, BC500, and BC1000. The BC500 fraction was then dialyzed against BD20 and subjected to a DEAE-5PW column (TosoHaas). The bound proteins were eluted with a 10-column-volumn (cv) linear gradient from BD20 to BD500. HMTase activities were separated into two peaks on this column. The first peak fractions were pooled and adjusted to BD500 using saturated ammonium sulfate and were then loaded onto a phenyl-Sepharose column (Pharmacia). The bound proteins were eluted with a 15-cv linear gradient from BD500 to BD0. HMTase activities were again split into two peaks. The fractions from both peaks were pooled separately and further fractionated following the same scheme described below. The pooled fractions were dialyzed into BC50 and then subjected to a Sephacryl S300 gel filtration column (Pharmacia). The HMTase activities eluted with a relative molecular mass of between 670 and 443 kDa from both pools. The fractions containing the HMTase activities were pooled, dialyzed against buffer P (5 mM HEPES-KOH [pH 7.5], 0.2 mM EDTA, 40 mM KCl, 0.01% Triton X-100, 0.01 mM $CaCl_2$, 1 mM DTT, 0.05 mM PMSF, and 10% glycerol) containing 10 mM potassium phosphate (BP10), and loaded onto a hydroxyapatite column. The bound proteins were eluted with a 12-cv linear gradient from BP10 to BP600. Fractions containing HMTase activity were combined and dialyzed into buffer BC150. The bound proteins were then eluted with a 10-cv linear gradient from BC150 to BC500. Finally, the active fractions were subjected to an affinity column containing protein A beads coated with SUZ12 antibodies to purify the EED-EZH2 complex. For protein identification, the candidate polypeptides were digested with trypsin and identified as previously described (28).

Purification of recombinant hPHF1-containing EED-EZH2 complex. hPHF1 cDNA was PCR amplified from an I.M.A.G.E cDNA clone, and the sequence was verified by DNA sequencing. The baculovirus construct was generated by insertion of the open reading frame of hPHF1 into the pFASTBAC vector (GIBCO) between the EcoRI and XhoI sites. The virus was generated and amplified according to the manufacturer's protocol. The baculoviruses for other components of the EED-EZH2 complex were previously described (4). The procedure for purification of the EED-EZH2 complex with or without hPHF1 was also described previously (4). The eluted complexes from the Flag affinity column were further purified over a gel-filtration Superose 6 column (Pharmacia).

HMTase assay and substrate preparations. Oligonucleosome, mononucleosome, and core histone substrates used for HMTase assays were purified from HeLa cells as described previously (4). Wild-type and mutant recombinant histone H3 were generated and purified as described previously (4). HMTase assays were performed essentially as previously described (28).

Kinetic analysis of the HMTase assay. The histone methylation assay was performed with a series of reactions containing increasing concentrations of ^{3}H-labeled *S*-adenosylmethionine (^{3}H-SAM). The reactions were allowed to proceed for 15 min and then stopped by addition of sodium dodecyl sulfate (SDS) loading buffer. Histones were separated by SDS-polyacrylamide gel electrophoresis (PAGE). Gels were exposed to film, and histone methylation was quantified by scintillation counting of bands containing histone 3 (H3) excised from gels. A histone sample with a known amount of radioactivity (cpm) was run at the same time to calibrate the incorporated methyl groups.

Plasmids and antibodies. Full-length hPHF1 cDNA was cloned into EcoRI and XhoI sites of pGEX-KG vector for the production of glutathione *S*-transferase (GST)-fusion protein. Antibodies against hPHF1 were generated in rabbit using hPHF1(230–567) as an antigen. Antibodies against SUZ12, H3K27me1, H3K27me2, H3K27me3, H3K4me2, and H3K9me3 have been previously described (4).

Generation and analysis of stable mPcl1 knockdown and Flag-mPcl1-rescued cell lines. 3T3 and GC1spg cells were cultured in Dulbecco's modified Eagle's medium supplemented with 10% fetal bovine serum at 37°C. The lentiviral vector pTY was requested from NIH AIDS Research & Reference Reagent Program and was modified by replacing LacZ with an internal ribosome entry site followed by either puromycin or enhanced green fluorescent protein (eGFP) for selection. The pTY-U6-mPcl1 small interfering RNA (siRNA) vector was cotransfected with pHP, pVSVG, and pCEP4tat into 293T cells with Superfect (Qiagen). The supernatant containing lentivirus was collected 36 h posttransfection and transduced into NIH 3T3 or GC1spg cells with 8 μg/ml Polybrene (Sigma). Stably transfected cells were selected in the presence of 2 μg/ml puromycin. To generate rescued cell lines, the stable KD cells were further transduced with lentiviruses expressing eGFP and Flag-mPcl1, which contains mutations on the siRNA targeting sequence. eGFP-positive cells were sorted by fluorescence-activated cell sorting and expanded for further analysis. RNAs were extracted from the above cell lines and analyzed by reverse transcription-PCR (RT-PCR) and real-time qPCR. The primer sequences for the Hox gene analysis were described previously (2). The oligonucleotides used to target mPcl1 mRNAs are RNA interference 1 (RNAi-1) sense primer GATGTGCTGGCCA GATGGA and antisense primer TCCATCTGGCGAGCACATC and RNAi-2 sense primer GGTCACCTCTGGGACTTCA and antisense primer TGAATG CCCAGAGGTGACC. The oligonucleotides used to target mEzh2 mRNAs are RNAi-1 sense primer GTATGTGGGCATCGAACGA and antisense primer TCGTTCGATGCCCACATAC. The primers used in the quantitative PCR (qPCR) were mPcl1 cDNA primers TGTTGTGTGTGTCGCTCTGA and AA ATGTCCAGCATCCCAGTC and mEzh2 cDNA primers AACCCTGTGACC ATCCACGGC and ATCAGACGGTGCCAGCAGTAAG. ChIP assays were performed with indicated antibodies as previously described (4). The primer pairs across the mouse Hox A10 genomic locus were designed by Array designer (Premierbiosoft) and listed as follows: 1, AAGTGTGTGAGCGAAAATTGTG and TCCAGCATTAACACAGTTTCAG; 2, TCTCCCAGGGATGGTGAA TCTC and ACTTGCTACCAGCCTCACAGAC; 3, AGTAGAGGCAGCCGT TGTAGTG and TCCTGAGCCGTCCCTGTCTG; 4, GCATAGCCTCCTGGG TGTGG and AGGCTGAGCTGGGTTTGGG; 5, AAATGGCTGGGAAAAG GACTGC and GCCGATGATCAATGCCTGGATC; 6, TGGCCTCGACTTA ACCTTCC and AACAAACACCAAGCAAACAGAC; 7, TCAGTGTCAAGT CCTGAATGGG and GAAGGATTTTAGCCAGGCAAGC; and 8, TCCATT TTATCCTGTCCACCAC and GTGGCCTAGCGGAGGACC. Platinum *Taq* polymerase (Invitrogen) and Sybr green master mix (Applied Bioscience) were used for PCR and real-time qPCR, respectively.

RESULTS

Purification and identification of an hPHF1-containing EED-EZH2 complex in HeLa cells. By monitoring HMTase activity, we previously purified and characterized an H3K27-specific methyltransferase EED-EZH2 complex (3). In the same purification, we noticed that the nucleosomal histone H3-specific methyltransferase activity split into two peaks on the DEAE-5PW column (Fig. 1B). From peak 2, we purified and characterized the EED-EZH2 complex, which contains

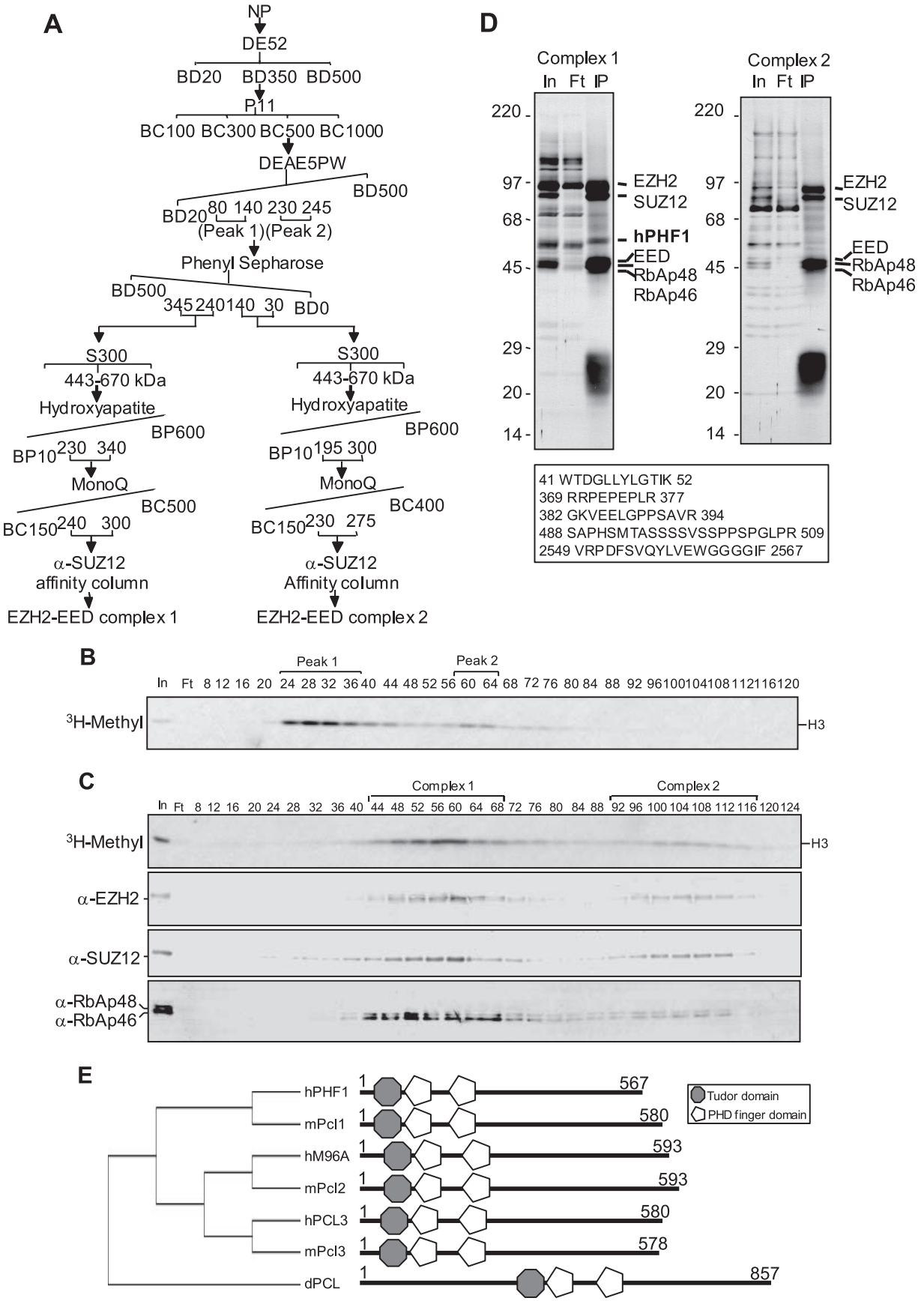
A
NP
DE52
BD20 BD350 BD500
P11
BC100 BC300 BC500 BC1000
DEAE5PW
BD500
BD20 80 140 230 245
(Peak 1)(Peak 2)
Phenyl Sepharose
BD500
345 240 140 30 BD0
S300
443-670 kDa
Hydroxyapatite
BP600
BP10 230 340
MonoQ
BC500
BC150 240 300
α-SUZ12
affinity column
EZH2-EED complex 1
S300
443-670 kDa
Hydroxyapatite
BP600
BP10 195 300
MonoQ
BC400
BC150 230 275
α-SUZ12
Affinity column
EZH2-EED complex 2
D
Complex 1
In Ft IP
Complex 2
In Ft IP
220
97
68
45
29
20
14
EZH2
SUZ12
hPHF1
EED
RbAp48
RbAp46
41 WTDGLLYLGTIK 52
369 RRPEPEPLR 377
382 GKVEELGPPSAVR 394
488 SAPHSMTASSSSVSSPPSPGLPR 509
2549 VRPDFSVQYLVEWGGGGIF 2567
B
Peak 1
Peak 2
In Ft 8 12 16 20 24 28 32 36 40 44 48 52 56 60 64 68 72 76 80 84 88 92 96 100 104 108 112 116 120
3H-Methyl
H3
C
Complex 1
Complex 2
In Ft 8 12 16 20 24 28 32 36 40 44 48 52 56 60 64 68 72 76 80 84 88 92 96 100 104 108 112 116 120 124
3H-Methyl
H3
α-EZH2
α-SUZ12
α-RbAp48
α-RbAp46
E
hPHF1
mPcl1
hM96A
mPcl2
hPCL3
mPcl3
dPCL
1
567
580
593
593
580
578
857
Tudor domain
PHD finger domain

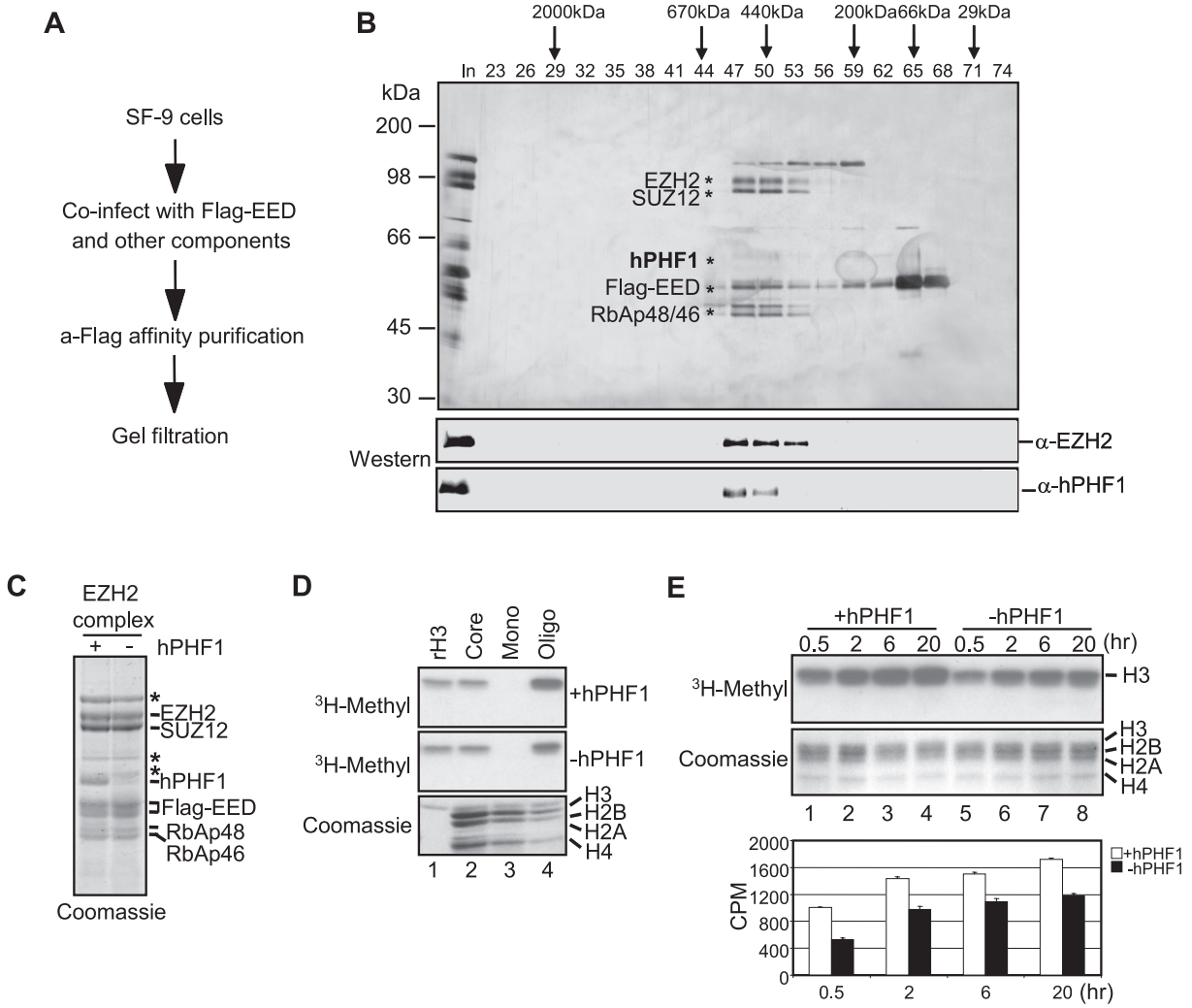

FIG. 2. Characterization of the hPHF1-containing EED-EZH2 complex in vitro. (A) Scheme for the steps carried out to reconstitute hPHF1-containing EED-EZH2 complex. a-Flag, anti-Flag. (B) Silver staining (top panel) and Western blotting (bottom panels) of the fractions derived from the Superose 6 gel-filtration column. The elution profile of the protein standards is indicated on top of the panel. The protein size markers are indicated to the left of the top panel. The antibodies (α-, anti-) used for Western blotting are indicated on the right. The six components of the reconstituted complex are indicated with asterisks. hPHF1 is stained weakly by silver. (C) Coomassie staining of a polyacrylamide-SDS gel containing the EED-EZH2 complexes in the presence or absence of hPHF1. Contaminating proteins from insect cells are indicated by asterisks. (D) Comparison of the substrate specificities of the two different recombinant EED-EZH2 complexes. Equal amounts of histone H3 alone or in octamer or mono- or oligonucleosome forms (bottom panel) were used as substrates for methylation by the two complexes shown in panel C (top two panels). (E) Time course experiment comparing the HMTase activities of the two complexes shown in panel C. A quantification of the top panel by scintillation counting is shown in the bottom panel.

EZH2, EED, SUZ12, RbAp48, and AEBP2 (3). To identify and characterize the enzymatic activity in peak 1, the proteins were fractionated on a phenyl Sepharose column, which further split the enzymatic activity into two peaks (Fig. 1C, top panel). Western blot analysis of the column fractions indicated that EZH2, SUZ12, RbAp48, and RbAp46 all cofractionate with the two enzymatic activities (Fig. 1C, bottom three panels). To define the composition of the two enzymatic activities,

FIG. 1. Purification and identification of hPHF1-containing EED-EZH2 complex. (A) Scheme used for purification of EED-EZH2 complexes. Numbers indicate the salt concentration (mM) at which the HMTase activity elutes from the respective columns. Nucleosomes were used as substrate in all of the HMTase assays. (B) HMTase activity assay of the fractions derived from the DEAE-5PW column. α-, anti-. (C) HMTase activity assay (top panel) and Western blot analysis (bottom panels) of fractions derived from the phenyl-Sepharose column. The antibodies used for Western blot analysis are indicated on the left side of the panel. (D) Silver staining of immunoprecipitated samples using antibodies against SUZ12. The positions of the protein size markers are indicated to the left of the panel. In, Ft, and IP represent input, flowthrough, and immunoprecipitates, respectively. The polypeptides copurified were identified by mass spectrometry, and their identities are indicated on the right. Representative peptides identified from mass spectrometry covering 41% of hPFH1 (GenBank accession no. BC008834) are shown in the box. (E) Phylogenetic tree of hPHF1 homologs from humans, mice, and flies. The relative positions of the conserved tudor domain and PHD domains are indicated. Numbers of amino acids for each protein are indicated.

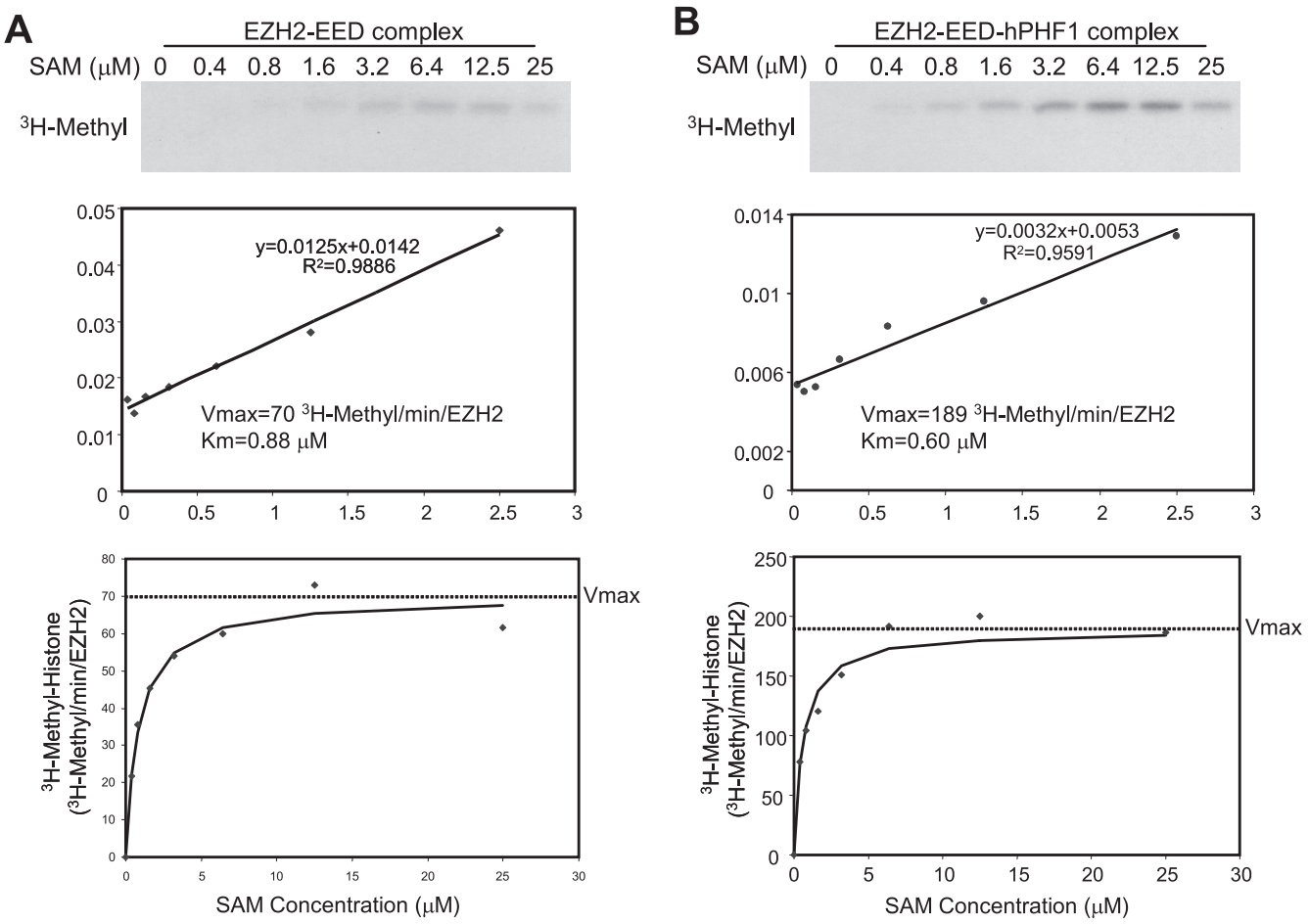

FIG. 3. Kinetic analysis of the EED-EZH2 complex in the presence or absence of hPHF1. Representative autoradiographs of HMTase assays containing different concentrations of ^{3}H-SAM are shown in the top panels. Lineweaver-Burk plots (or double-reciprocal plots) of the reactions are shown in the middle panels. V_{max} and K_m were determined and are indicated on the plots. Michaelis-Menten plots were generated and are shown in the bottom panels. EED-EZH2 complex in the absence or presence of hPHF1 was used as the enzyme in panels A and B, respectively.

the samples were further fractionated sequentially on S300, hydroxyapatite, and MonoQ columns before being affinity purified using an anti-SUZ12 antibody column (Fig. 1A). Silver staining followed by mass spectrometry analysis of the affinity purified samples indicated that both enzymatic protein complexes contain EZH2, SUZ12, EED, RbAp48, and RbAp46. However, hPHF1 was only present in complex 1 (Fig. 1D).

Sequence analysis indicated that hPHF1 is highly related to the *Drosophila* PcG protein PCL. The fly Pcl gene was identified in a genetic screen as an enhancer of Polycomb (Pc), and both homozygous and heterozygous mutants exhibit lethal and homeotic phenotypes (7). Previous studies have demonstrated that the *Drosophila* PCL protein associates with the ESC-E(Z) complex during early embryogenesis and can directly interact with E(Z) through its PHD fingers (21, 26). In contrast to *Drosophila*, where only a single Pcl gene exists, three genes that code for protein homologs to fly Pcl have been identified in both human and mouse genomes (Fig. 1E). hPHF1 was mapped to chromosome 6p21.3 by fluorescence in situ hybridization and shows 42% similarity to *Drosophila* Pcl (5). Its closest mouse homolog, mPcl1, originally named Tctex3 (T-complex testis expressed 3), is expressed specifically in the testis (12), but its function remains unknown. mPcl2 was initially cloned as a metal response transcription factor, Mtf2/M96 (11). Loss of functional mutation in mice causes posterior transformation of axial skeletons with low penetrance that is less severe than the defects exhibited with Pcl mutation in *Drosophila*, indicating that there might be functional redundancy among the Pcl homologs in mice (30). hPCL3 was first identified in humans and has been shown to be upregulated in multiple cancers (31). The function and expression pattern of mPcl3 remain to be characterized.

hPHF1 stimulates the enzymatic activity of the EED-EZH2 complex by affecting the reaction V_{max} and K_m. To assess the potential role of hPHF1 in modulating the enzymatic activity of EED-EZH2 complex, we reconstituted the EED-EZH2 complex in the presence or absence of hPHF1 following the scheme outlined in Fig. 2A. A homogenous EED-EZH2 complex with hPHF1 was purified by affinity chromatography followed by gel filtration to remove unincorporated free Flag-EED and Flag-EED-containing subcomplexes (Fig. 2B). Silver staining and Western blot analysis of the column fractions confirmed that hPHF1 copurifies with other components in a protein complex between 440 and 670 kDa, which behaves

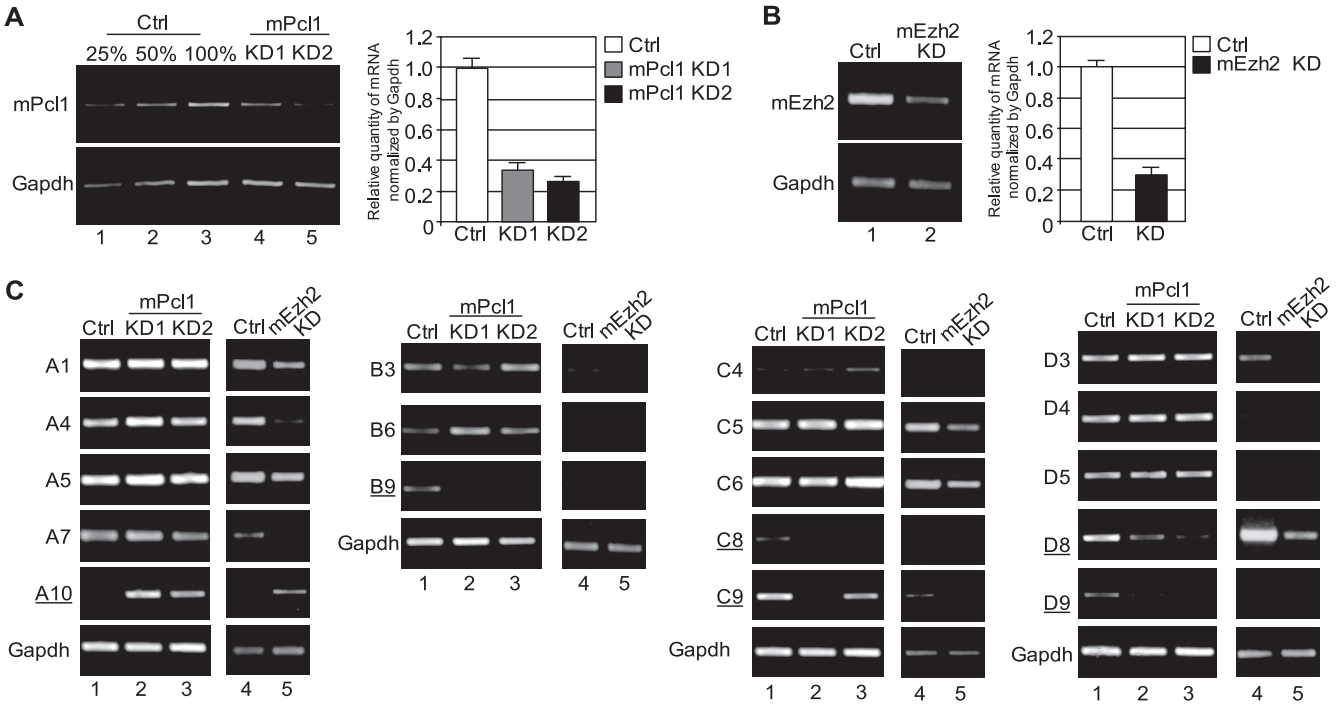

FIG. 4. Knockdown of mPcl1 and Ezh2 in NIH 3T3 cells affects Hox gene expression. (A) Characterization of the stable mPcl1 knockdown cell lines by RT-PCR (left panel) and RT-qPCR (right panel). Glyceraldehyde-3-phosphate dehydrogenase (GAPDH) was used as control (Ctrl) in both experiments. (B) Characterization of a stable Ezh2 knockdown cell lines by RT-PCR (left panel) and RT-qPCR (right panel). GAPDH was used as a control. (C) RT-PCR analysis of Hox gene expression pattern in response to knockdown of mPcl1 (lanes 2 and 3) or Ezh2 (lane 5). GAPDH serves as a control for equal input. The Hox genes affected by knockdown of mPcl1 or Ezh2 are underlined.

similarly to the native complex (Fig. 1A). Using the same strategy, we also reconstituted and purified a complex without hPHF1 (Fig. 2C). We note that hPHF1 is not stained well by silver (Fig. 2B) but is readily detected by Coomassie staining (Fig. 2C).

Previous studies indicated that the EED-EZH2 complex prefers oligonucleosome substrates (4). To test whether incorporation of hPHF1 in the EED-EZH2 complex affects its substrate preference, equal amounts of histone H3 in various forms were subjected to methylation by equal amounts of EED-EZH2 complex in the presence or absence of hPHF1. The results shown in Fig. 2D indicate that incorporation of hPHF1 might increase its relative activity for oligonucleosome substrates. In addition, a time course experiment demonstrated that incorporation of hPHF1 into the complex improved the kinetics of the methylation reaction (Fig. 2E). However, incorporation of hPHF1 does not change the site specificity (H3K27) of the EED-EZH2 complex (data not shown).

To understand the exact effect of hPHF1 on the reaction kinetics, we performed methyltransferase reactions using a wide range of SAM concentrations and allowed the reaction to proceed for only 15 min to keep it in the linear range (Fig. 3). The maximal velocity (V_{max}) and the Michaelis-Menten constant (K_m) were then derived from the Lineweaver-Burk plot (or double-reciprocal plot) (Fig. 3, middle panels). Based on the calculated V_{max} and K_m, accurate Michaelis-Menten plots were generated. This analysis revealed that incorporation of hPHF1 increased the reaction V_{max} from 70 to 189 methyl histones/min/enzyme, while it decreased the K_m from 0.88 to 0.60 μM. Together, these data allow us to conclude that hPHF1 stimulates the activity of EED-EZH2 complex by increasing the V_{max} 2.7-fold and decreasing the K_m 1.5-fold.

Knockdown of mPcl1 affects Hox gene expression. To assess the function of hPHF1 in H3K27 methylation in vivo, we used a lentivirus-derived siRNA approach in NIH 3T3 cells to generate two stable knockdown cell lines, KD1 and KD2, which target the N-terminal or C-terminal region of mPcl1, respectively. Semiquantitative and real-time RT-PCR analysis demonstrated over 60 to 70% reduction in the mRNA levels of the two knockdown cell lines (Fig. 4A). Because mPcl1 only presents in a subpopulation of the Eed-Ezh2 complexes, we also generated a stable Ezh2 knockdown cell line using a similar strategy for purposes of comparison. Characterization of the Ezh2 knockdown cell line by semiquantitative and real-time RT-PCR indicates that about 70% knockdown at the mRNA level was achieved (Fig. 4B). To evaluate the respective effects of mPcl1 and Ezh2 knockdown on Hox gene expression, we analyzed the expression levels of all 39 mouse Hox genes in the knockdown cells and compared them to that in the control cells by RT-PCR. Due to the low expression levels of some Hox genes in NIH 3T3 cells, we were able to detect expression of only 18 Hox genes. Results shown in Fig. 4C indicate that Ezh2 knockdown resulted in a broad and significant change in Hox gene expression. In contrast, knockdown of mPcl1 only affected expression of a limited number of genes. Interestingly, most genes that are affected by mPcl1 knockdown are downregulated, but HoxA10 is up-regulated in response to Ezh2 and

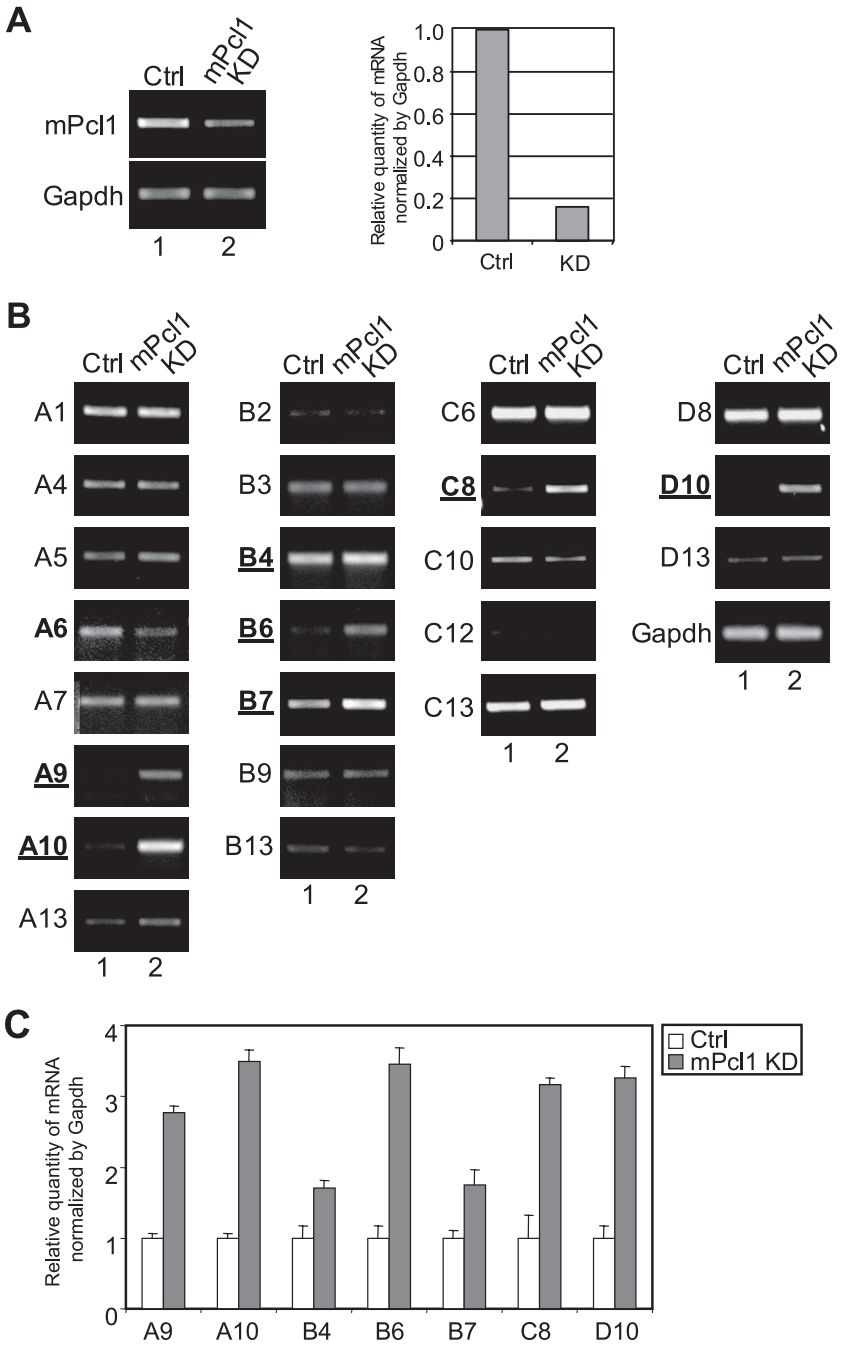

FIG. 5. Knockdown of mPcl1 in GC1Spg cells affects Hox gene expression. (A) Characterization of the stable mPcl1 knockdown cell lines by RT-PCR (left panel) and RT-qPCR (right panel). Glyceraldehyde-3-phosphate dehydrogenase (GAPDH) was used as a control (Ctrl) in both experiments. (B) RT-PCR analysis of Hox gene expression pattern in response to knockdown of mPcl1 relative to control. GAPDH serves as a control for equal input. The Hox genes whose expression is affected by mPcl1 knockdown are underlined. (C) RT-qPCR analysis of selected genes affected by mPcl1 knockdown shown in panel B. Results are normalized to GAPDH and are presented as means ± standard deviations from two independent experiments.

mPcl1 knockdown. Given that PcG proteins are known to be involved in transcriptional silencing, genes that are down-regulated by Ezh2 or mPcl1 knockdown might be a result of indirect effects.

Because very few Hox genes analyzed are affected by mPcl1 knockdown in NIH 3T3 cells, it is possible that NIH 3T3 is not the appropriate cell type for analysis of mPcl1 function. Since mPcl1 (also named Tctex3) was first identified due to its unique and restricted expression pattern in male germ cells (12), we speculated that knockdown of mPcl1 in male germ cells might cause a broader effect on Hox gene expression. Therefore, we generated knockdown of mPcl1 in GC1Spg cells, an immortalized mouse male germ cell line that constitutively expresses the simian virus 40 large T antigen (15),

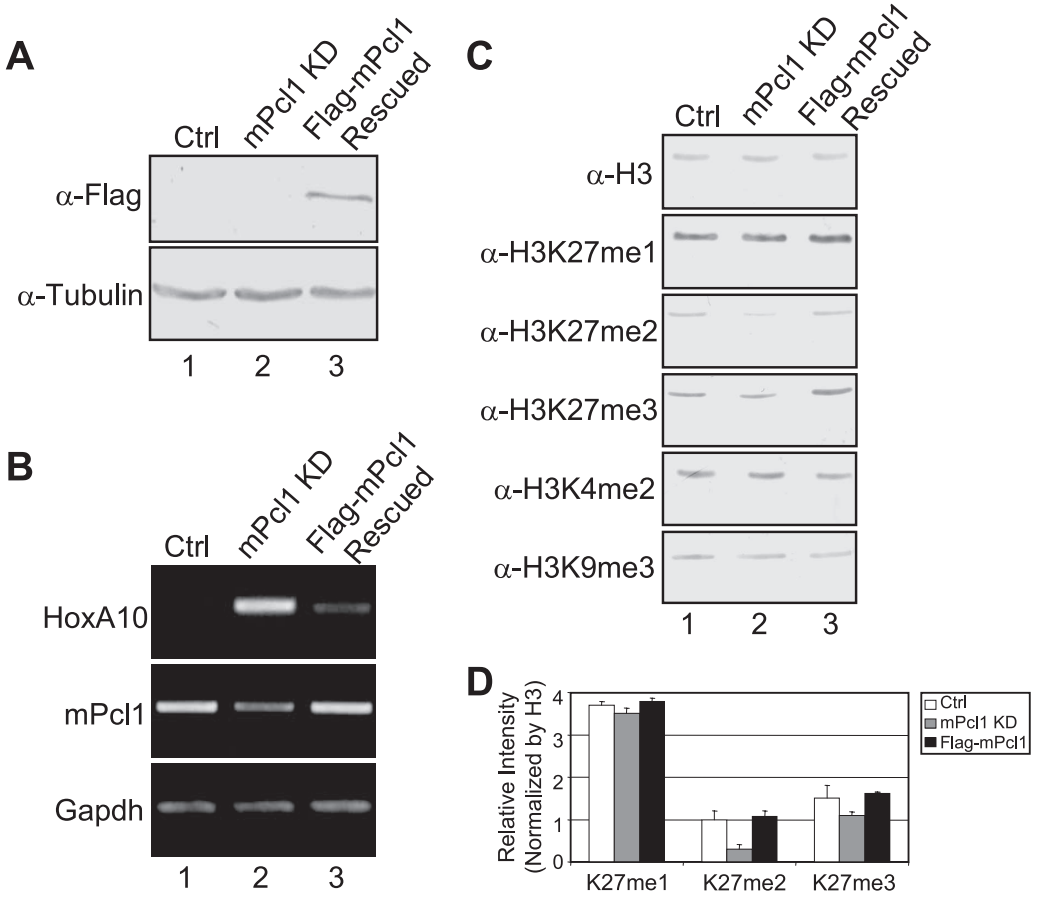

FIG. 6. HoxA10 is a direct target of mPcl1. (A) Characterization of a stable Flag-mPcl1-rescued cell line by Western blotting. Equal loading was confirmed by Western blotting using α-tubulin antibody. α-Flag, anti-Flag antibody; Ctrl, control. (B) RT-PCR analysis of HoxA10 and mPcl1 expression in mock, mPcl1 knockdown, and Flag-mPcl1-rescued cell lines. Glyceraldehyde-3-phosphate dehydrogenase (GAPDH) served as a control for equal input. (C) Western blot analysis of histone extracts from control, knockdown, and Flag-mPcl1-rescued cell lines. The antibodies used are indicated. Equal loading was verified by antibody against histone H3 (top panel). (D). Quantitative analysis of the changes of mono-, di-, and trimethylation shown in panel C by Licor image software. The data were normalized with total histone H3 and are presented as relative intensity from three independent experiments.

using the KD2 lentivirus-delivered siRNA. Expectedly, more efficient knockdown was achieved in this cell line, with a more than 80% reduction in the mRNA level as determined by real-time PCR (Fig. 5A). Interestingly, the expression levels of multiple Hox genes were altered and most of them, including HoxA10, are upregulated by knockdown of mPcl1 (Fig. 5B and C). Because a higher knockdown efficiency for mPcl1 and a broader effect on Hox gene expression are observed in the GC1spg cell line, we performed further analysis of mPcl1 function in this cell line. Because mPcl1 knockdown resulted in significant up-regulation of the HoxA10 gene in two different cell lines, subsequent analysis was focused on this gene.

Pcl1 contributes to H3K27me2 and H3K27me3 level in vivo. To exclude possible off-target effects of mPcl1 knockdown and to overcome the problem that no Pcl1 antibody capable of working for ChIP is available, we generated a cell line that stably expresses Flag-mPcl1 using the GC1spg-derived Pcl1 knockdown cell line (Fig. 6A). RT-PCR analysis indicated that the expression of Flag-mPcl1 restored the mPcl1 level to that of the control (Fig. 6B, middle panel). Importantly, rescue of mPcl1 knockdown resulted in recovery of HoxA10 silencing (Fig. 6B, top panel), demonstrating that mPcl1 plays an important role in HoxA10 silencing. To address whether mPcl1 knockdown affects the global H3K27 methylation level, we compared the H3K27 methylation levels of histones isolated from control, knockdown, and rescued cell lines. Results shown in Fig. 6C indicate that mPcl1 knockdown results in a global decrease in H3K27me2 and H3K27me3 levels but has no obvious effects on the levels of other modifications, such as H3K27me1, H3K4me2, or H3K9me3 (Fig. 6C, lanes 1 and 2). Quantification of the methylation levels indicates that knockdown of mPcl1 resulted in decreases of genome-wide H3K27 di- and trimethylation levels to 30% and 70% of the control levels, respectively (Fig. 6D). Apparently this effect is directly related to mPcl1 knockdown, as rescue of mPcl1 expression by Flag-mPcl1 restored the H3K27 methylation levels (Fig. 6C and D).

Binding of mPcl1 to HoxA10 correlates to increased H3K27me2 level and HoxA10 silencing. To further characterize the relationship between mPcl1 binding, H3K27 methylation and HoxA10 silencing, we performed ChIP analysis across the entire HoxA10 gene using control, mPcl1 knock-

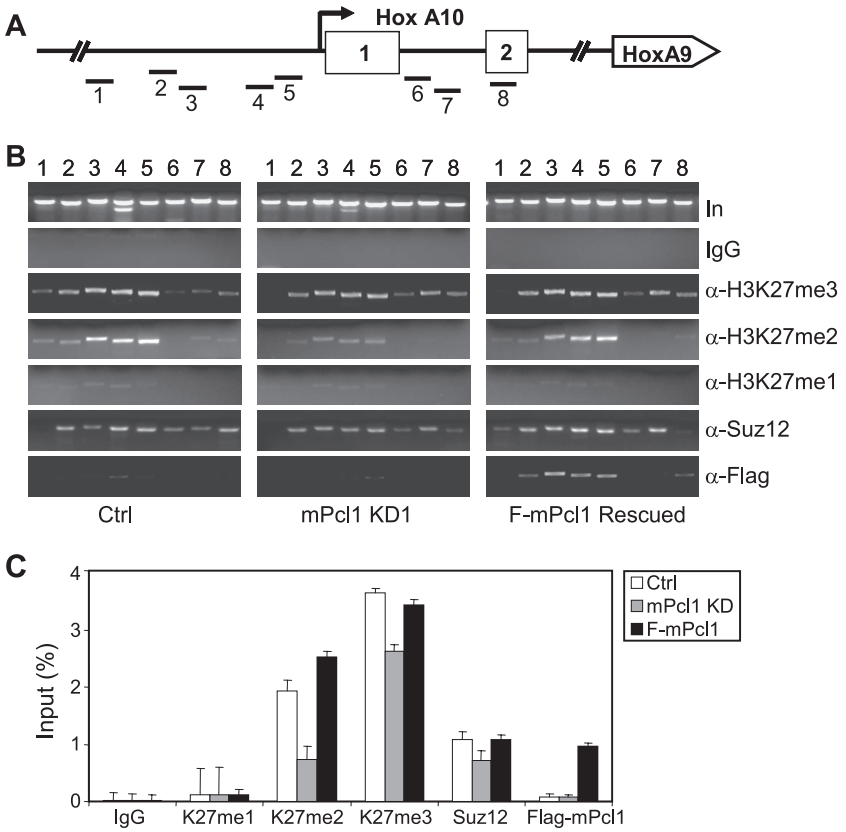

FIG. 7. mPcl1 knockdown leads to a decreased H3K27me2 level at the promoter region, which can be rescued by expression of Flag-mPcl1. (A) Diagram of the HoxA10 gene in which the two exons are indicated by boxes labeled with 1 and 2. The regions analyzed are indicated with bars and are labeled from 1 to 8. Each region covers about 500 bp. (B) ChIP analysis of the HoxA10 gene using various antibodies (α-, anti-) indicated on the right. The cell lines used in ChIP are indicated at the bottom of each panel. The different amplicons analyzed are indicated on top of the panel. Ctrl, control. (C). ChIP-qPCR analysis of the relative levels of mono-, di-, and trimethylation of H3K27, Suz12, and Flag-mPcl1 on region 4 shown in panel A. Results are shown as percentages of enrichment relative to input. The data shown represent means ± standard deviations from two independent experiments.

down, and Flag-mPcl1-rescued cells. Antibodies used for ChIP assays include anti-Suz12, anti-Flag, and all three forms of anti-H3K27me. An equal amount of IgG was used as a control for antibody specificity. Results shown in Fig. 7B indicate that Flag-mPcl1 is localized to the promoter and upstream flanking region (amplicons 3 to 5; bottom panel). H3K27me2 and H3K27me3 levels are also enriched in the same region in the Flag-mPcl-rescued cells compared to that in the knockdown cells. However, H3K27me1 signal was not detected in all regions examined. Interestingly, knockdown of mPcl1 resulted in a significant decrease in H3K27me2 levels, while only a mild decrease in H3K27me3 levels is observed (Fig. 7B, compare left and middle panels). Notably, in region 4 and the surrounding region, H3K27 dimethylation and trimethylation were decreased to less than 40% and 70%, respectively (Fig. 7C). Importantly, the decreased H3K27 methylation caused by mPcl1 knockdown was restored to the control level in the rescued cells (Fig. 7B and C). Moreover, knockdown of mPcl1 appears to cause a subtle, but consistent, decrease in binding of Suz12 to the promoter region (Fig. 7B, amplicons 4 and 5, and C), which is also restored in the rescue cells (Fig. 7B, amplicons 4 and 5, and C). mPcl1 binding appears to correlate with Suz12 recruitment and H3K27 methylation. This raises the possibility that mPcl1 may contribute to Eed-Ezh2 recruitment to a subset of Hox genes. This possibility is consistent with a previous study demonstrating a direct interaction between the PHD domains of *Drosophila* PCL and E(Z) (21).

DISCUSSION

Drosophila PCL was initially identified in a yeast two-hybrid screen as an interaction partner of E(Z) (21). This interaction was later confirmed by the isolation of a 1-MDa protein complex from *Drosophila* embryo extracts that contains all of the core components of the ESC-E(Z) complex, as well as PCL and RPD3, a histone deacetylase (26). In this study, we provide evidence that one of the human homologs of PCL, hPHF1 associates with the core components of the EED-EZH2 complex and has the capacity to modulate its enzymatic activity and Hox gene expression. By comparing the enzymatic activity of a native *Drosophila* PCL-containing complex and a reconstituted ESC-E(Z) complex, another group recently suggested that PCL might enhance the enzymatic activity of the ESC-E(Z) complex (19). Given that the study failed to reconstitute a PCL-containing complex, it cannot rule out the possibility that the observed difference in enzymatic activities is caused by

differences in the native and reconstituted complexes other than PCL. In contrast, by comparing the reconstituted complexes in the presence or absence of hPHF1 directly, we revealed a potential role for hPHF1 in modulating the enzymatic activity of the EED-EZH2 complex.

To understand the molecular mechanism by which hPHF1/mPcl1 affects H3K27 methylation and Hox gene silencing, we put significant effort into characterizing the conserved PHD and tudor domains that are present in the hPHF1 protein. Given that both PHD and tudor domains have been recently demonstrated to have the capacity of binding to methylated histones (10, 24, 32), we explored the possibility that hPHF1 may bind to a specifically methylated histone lysine residue by a variety of approaches. These attempts failed to generate any convincing data supporting recognition of any methylated lysine residues on histones by hPHF1 (data not shown). Furthermore, deletion of the second PHD domain, which contains the most conserved aromatic residues predicted to be potential methyl-lysine recognition sites, does not affect the ability of Flag-mPcl1 to rescue the altered Hox gene expression in response to mPcl1 knockdown (data not shown). These results do not support that recognition of methylated histone lysine residues is the underlying mechanism for hPHF1 to stimulate the EED-EZH2 methyltransferase activity and Hox gene silencing. However, hPHF1 does appear to recognize a specific feature of nucleosomes, as it can interact with nucleosomes in vitro (data not shown). This property, in combination with the fact that PCL interacts directly with E(Z) (21), may explain why hPHF1 can stimulate the enzymatic activity of the EED-EZH2 complex.

In *Drosophila*, homozygous *Pcl* mutant embryos exhibit variable short-range transformation toward the posterior, while the anterior segments remain unaffected. This phenotype is different from those exhibited by other PcG mutants such as those with mutation of *Pc* or *Esc*, suggesting that they each may have some unique functions (7, 25). Consistent with this observation, removal of PCL in embryos or in imaginal discs only decreased, but did not abolish, H3K27 trimethylation, which is different from inactivation of E(Z). Moreover, Pcl mutants also exhibit increased H3K27me1 and H3K27me2 levels concomitant with a decrease in H3K27me3 levels and Su(z)12 recruitment, suggesting that PCL might be only required for generating the H3K27me3 mark at its target genes. However, it is not clear how PCL achieves this effect (19). Several pieces of evidence suggest that PCL and its homologs may have some tissue-specific functions. For example, analysis of maternal and zygotic *Pcl* mutants indicated that while only moderate misexpression of Hox genes was observed in the epidermis, much broader and stronger misexpression of Hox genes was observed in the viscera mesoderm and central nervous system (25). Similarly, analysis of a PCL homolog in *Xenopus* also revealed specific function in neuronal development (33). This suggests that unlike the core components of the ESC-E(Z) complex, which strongly repress Hox gene expression in all tissues, PCL only regulates a subset of Hox genes in a tissue-specific manner. Consistent with this notion, our analysis in NIH 3T3 cells revealed that knockdown of mPcl1 affects expression of only a few Hox genes, while knockdown of Ezh2 alters expression of many Hox genes. However, when similar experiments are performed in a mouse germ cell line, mPcl1 knockdown exhibits a much broader effect. Therefore, PCL and its mammalian homologs might be important in defining tissue-specific function of the EED-EZH2 complex. Future work should be able to determine whether this is indeed the case.

ACKNOWLEDGMENTS

We thank Kathryn Gardner for reading the manuscript.

This work was partly supported by grant GM68804 (to Y.Z.), and P30 CA08748 (to P.T.). Y.Z. is an Investigator of the Howard Hughes Medical Institute.

REFERENCES

1. **Buchwald, G., P. van der Stoop, O. Weichenrieder, A. Perrakis, M. van Lohuizen, and T. K. Sixma.** 2006. Structure and E3-ligase activity of the Ring-Ring complex of polycomb proteins Bmi1 and Ring1b. EMBO J. **25:** 2465–2474.
2. **Cao, R., Y. I. Tsukada, and Y. Zhang.** 2005. Role of Bmi-1 and Ring1A in H2A ubiquitylation and Hox gene silencing. Mol. Cell **20:**845–854.
3. **Cao, R., L. Wang, H. Wang, L. Xia, H. Erdjument-Bromage, P. Tempst, R. S. Jones, and Y. Zhang.** 2002. Role of histone H3 lysine 27 methylation in Polycomb-group silencing. Science **298:**1039–1043.
4. **Cao, R., and Y. Zhang.** 2004. SUZ12 is required for both the histone methyltransferase activity and the silencing function of the EED-EZH2 complex. Mol. Cell **15:**57–67.
5. **Coulson, M., S. Robert, H. J. Eyre, and R. Saint.** 1998. The identification and localization of a human gene with sequence similarity to Polycomblike of Drosophila melanogaster. Genomics **48:**381–383.
6. **Czermin, B., R. Melfi, D. McCabe, V. Seitz, A. Imhof, and V. Pirrotta.** 2002. Drosophila Enhancer of Zeste/ESC complexes have a histone H3 methyltransferase activity that marks chromosomal Polycomb sites. Cell **111:**185–196.
7. **Duncan, I. M.** 1982. Polycomblike: a gene that appears to be required for the normal expression of the bithorax and antennapedia gene complexes of Drosophila melanogaster. Genetics **102:**49–70.
8. **Fischle, W., Y. Wang, S. A. Jacobs, Y. Kim, C. D. Allis, and S. Khorasanizadeh.** 2003. Molecular basis for the discrimination of repressive methyl-lysine marks in histone H3 by Polycomb and HP1 chromodomains. Genes Dev. **17:**1870–1881.
9. **Francis, N. J., and R. E. Kingston.** 2001. Mechanisms of transcriptional memory. Nat. Rev. Mol. Cell Biol. **2:**409–421.
10. **Huang, Y., J. Fang, M. T. Bedford, Y. Zhang, and R. M. Xu.** 2006. Recognition of histone H3-lysine 4 methylation by the double tudor domain of JMJD2A. Science **312:**748–751.
11. **Inouye, C., P. Remondelli, M. Karin, and S. Elledge.** 1994. Isolation of a cDNA encoding a metal response element binding protein using a novel expression cloning procedure: the one hybrid system. DNA Cell Biol. **13:** 731–742.
12. **Kawakami, S., K. Mitsunaga, Y. Y. Kikuti, A. Ando, H. Inoko, K. Yamamura, and K. Abe.** 1998. Tctex3, related to Drosophila polycomblike, is expressed in male germ cells and mapped to the mouse t-complex. Mamm. Genome **9:**874–880.
13. **Kuzmichev, A., K. Nishioka, H. Erdjument-Bromage, P. Tempst, and D. Reinberg.** 2002. Histone methyltransferase activity associated with a human multiprotein complex containing the Enhancer of Zeste protein. Genes Dev. **16:**2893–2905.
14. **Li, Z., R. Cao, M. Wang, M. P. Myers, Y. Zhang, and R.-M. Xu.** 2006. Structure of a Bmi-1-Ring1B Polycomb group ubiquitin ligase complex. J. Biol. Chem. **281:**20643–20649.
15. **Luers, G. H., A. Schad, H. D. Fahimi, A. Volkl, and J. Seitz.** 2003. Expression of peroxisomal proteins provides clear evidence for the presence of peroxisomes in the male germ cell line GC1spg. Cytogenet. Genome Res. **103:**360–365.
16. **Min, J., Y. Zhang, and R. M. Xu.** 2003. Structural basis for specific binding of Polycomb chromodomain to histone H3 methylated at Lys 27. Genes Dev. **17:**1823–1828.
17. **Montgomery, N. D., D. Yee, A. Chen, S. Kalantry, S. J. Chamberlain, A. P. Otte, and T. Magnuson.** 2005. The murine polycomb group protein Eed is required for global histone H3 lysine-27 methylation. Curr. Biol. **15:**942–947.
18. **Muller, J., C. M. Hart, N. J. Francis, M. L. Vargas, A. Sengupta, B. Wild, E. L. Miller, M. B. O'Connor, R. E. Kingston, and J. A. Simon.** 2002. Histone methyltransferase activity of a Drosophila polycomb group repressor complex. Cell **111:**197–208.
19. **Nekrasov, M., T. Klymenko, S. Fraterman, B. Papp, K. Oktaba, T. Kocher, A. Cohen, H. G. Stunnenberg, M. Wilm, and J. Muller.** 2007. Pcl-PRC2 is needed to generate high levels of H3-K27 trimethylation at Polycomb target genes. EMBO J. **26:**4078–4088.
20. **Nekrasov, M., B. Wild, and J. Muller.** 2005. Nucleosome binding and histone methyltransferase activity of Drosophila PRC2. EMBO Rep. **6:**348–353.

21. **O'Connell, S., L. Wang, S. Robert, C. A. Jones, R. Saint, and R. S. Jones.** 2001. Polycomblike PHD fingers mediate conserved interaction with enhancer of zeste protein. J. Biol. Chem. **276:**43065–43073.
22. **Pasini, D., A. P. Bracken, M. R. Jensen, E. Lazzerini Denchi, and K. Helin.** 2004. Suz12 is essential for mouse development and for EZH2 histone methyltransferase activity. EMBO J. **23:**4061–4071.
23. **Saurin, A. J., Z. Shao, H. Erdjument-Bromage, P. Tempst, and R. E. Kingston.** 2001. A Drosophila Polycomb group complex includes Zeste and dTAFII proteins. Nature **412:**655–660.
24. **Shi, X., T. Hong, K. L. Walter, M. Ewalt, E. Michishita, T. Hung, D. Carney, P. Pena, F. Lan, M. R. Kaadige, N. Lacoste, C. Cayrou, F. Davrazou, A. Saha, B. R. Cairns, D. E. Ayer, T. G. Kutateladze, Y. Shi, J. Cote, K. F. Chua, and O. Gozani.** 2006. ING2 PHD domain links histone H3 lysine 4 methylation to active gene repression. Nature **442:**96–99.
25. **Soto, M. C., T. B. Chou, and W. Bender.** 1995. Comparison of germline mosaics of genes in the Polycomb group of Drosophila melanogaster. Genetics **140:**231–243.
26. **Tie, F., J. Prasad-Sinha, A. Birve, Å. Rasmuson-Lestander, and P. J. Harte.** 2003. A 1-megadalton ESC/E(Z) complex from *Drosophila* that contains Polycomblike and RPD3. Mol. Cell. Biol. **23:**3352–3362.
27. **Verreault, A., P. D. Kaufman, R. Kobayashi, and B. Stillman.** 1998. Nucleosomal DNA regulates the core-histone-binding subunit of the human Hat1 acetyltransferase. Curr. Biol. **8:**96–108.
28. **Wang, H., Z. Q. Huang, L. Xia, Q. Feng, H. Erdjument-Bromage, B. D. Strahl, S. D. Briggs, C. D. Allis, J. Wong, P. Tempst, and Y. Zhang.** 2001. Methylation of histone H4 at arginine 3 facilitating transcriptional activation by nuclear hormone receptor. Science **293:**853–857.
29. **Wang, H., L. Wang, H. Erdjument-Bromage, M. Vidal, P. Tempst, R. S. Jones, and Y. Zhang.** 2004. Role of histone H2A ubiquitination in Polycomb silencing. Nature **431:**873–878.
30. **Wang, S., F. He, W. Xiong, S. Gu, H. Liu, T. Zhang, X. Yu, and Y. Chen.** 2007. Polycomblike-2-deficient mice exhibit normal left-right asymmetry. Dev. Dyn. **236:**853–861.
31. **Wang, S., G. P. Robertson, and J. Zhu.** 2004. A novel human homologue of Drosophila polycomblike gene is up-regulated in multiple cancers. Gene **343:**69–78.
32. **Wysocka, J., T. Swigut, H. Xiao, T. A. Milne, S. Y. Kwon, J. Landry, M. Kauer, A. J. Tackett, B. T. Chait, P. Badenhorst, C. Wu, and C. D. Allis.** 2006. A PHD finger of NURF couples histone H3 lysine 4 trimethylation with chromatin remodelling. Nature **442:**86–90.
33. **Yoshitake, Y., T. L. Howard, J. L. Christian, and S. M. Hollenberg.** 1999. Misexpression of Polycomb-group proteins in Xenopus alters anterior neural development and represses neural target genes. Dev. Biol. **215:**375–387.